Quantum Processing of Images by Continuous Wave Optical Parametric Amplification

L. Lopez,[1] N. Treps,[1] B. Chalopin,[1] C. Fabre,[1] and A. Maître[1,2]

[1]*Laboratoire Kastler Brossel, Université Pierre et Marie Curie-Paris 6, École Normale Supérieure, CNRS, CC74, 4 Place Jussieu, 75252 Paris CEDEX 05, France*

[2]*Institut des NanoSciences de Paris, Université Pierre et Marie Curie-Paris 6, CNRS, Campus Boucicaut, 140 rue de Lourmel, 75015 Paris, France*

(Received 22 December 2006; published 10 January 2008)

We have experimentally shown that a degenerate optical parametric oscillator pumped by a cw laser, inserted in a cavity having degenerate transverse modes such as a hemiconfocal or confocal cavity, and operating below the oscillation threshold in the regime of phase sensitive amplification, is able to process input images of various shapes in the quantum regime. More precisely, when deamplified, the image is amplitude squeezed; when amplified, its two polarization components are intensity correlated at the quantum level. In addition, the amplification process of the images is shown to take place in the noiseless regime.

DOI: 10.1103/PhysRevLett.100.013604 PACS numbers: 42.50.Dv, 42.60.Da, 42.65.Yj

In order to be really useful quantum information processing devices will have to process simultaneously a great number of quantum variables and will have therefore to operate in a Hilbert space of high dimensionality. In the discrete variable regime this is achieved by processing simultaneously many qubits carried by different quantum objects [1]. In the continuous variable regime, this will be achieved by working in a highly multimode system, described by a great number of continuous quantum variables. In this respect, optical images are of high interest, as they carry in an intrinsically parallel way a great quantity of information [2]. In addition, decoherence can be very low in such systems. It is therefore of great importance for future applications to develop experimental techniques that are able to process images at the quantum level, i.e., with a minimum amount of added quantum noise in order to minimize errors in the quantum channel.

The second interest of dealing with images at the quantum level is in the domain of ''quantum metrology,'' i.e., in the improvement by quantum techniques of measurements performed in optical images, and more generally of information extraction through image processing [3]. It was theoretically demonstrated that the reduction of local quantum fluctuations in the transverse plane of an image, or the generation of quantum correlations between different parts of the image, leads to such an improvement. To obtain it, one needs to squeeze the ''noise mode'' of the measurement, i.e., generate a squeezed state in a well-defined mode that can have a complicated transverse shape. This was experimentally implemented in the case of ''nanopositioning'' [4], which required the generation of squeezed light either in a ''flipped mode,'' having a π phase shift between its two halves, or in a TEM_{01} mode. The interest of using squeezed states in modes of complicated shapes was also outlined in the issue of optical readout of information stored on supports like CDs and DVDs, but containing much more than 1 bit of information per λ^2 [5,6].

Degenerate parametric amplification is a very convenient tool to generate light beams of adjustable transverse variation having nonclassical local fluctuations and spatial correlations: fed by an input coherent state, it amplifies it in a noiseless way [7] and can generate at the output either squeezed states or ''quantum clones'' [8]. This has been experimentally observed in single pass parametric amplification using an intense pulsed laser as a pump. In [8] the input field was in the TEM_{00} transverse mode. The first experiment of processing at the quantum level a more complicated image was reported in [9], and used a double slit as an input image. Pulsed parametric amplification was also recently used to demonstrate noiseless amplification for quantum spatial fluctuations [10]. Other nonlinear processes could also be used in this purpose, such as four-wave mixing in atomic vapors [11] or active feedforward schemes [12].

In view of applications, and especially for quantum metrology in images, it is very important to be able to operate a parametric amplifier in the continuous regime, for which are available low noise and stable sources of light that are well suited to high sensitivity measurements. We report in this Letter the first experimental demonstration of cw amplification of images in the quantum regime. This has been achieved using frequency-degenerate parametric amplification inside a resonant cavity. This device is a well known cw source of squeezed vacuum [13], bright squeezed light [14], EPR light [15], and can operate as a noiseless amplifier [16], but only so far for the TEM_{00} eigenmode of the cavity [17]. In order to generate nonclassical images with more complex shapes, we have used cavities that do not impose the transverse variation of the light amplitude, i.e., transverse degenerate cavities, such as confocal or hemiconfocal cavities, in which an infinite number of transverse modes are simultaneously resonant.

The experimental setup is depicted in Fig. 1. It uses a cw, frequency doubled, Nd:Yag laser with two coherent out-

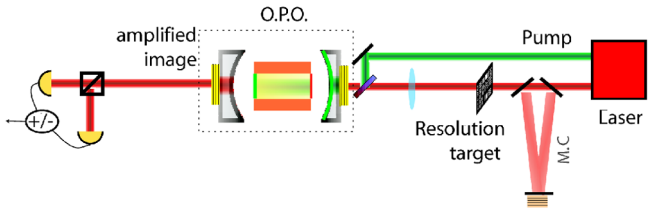

FIG. 1 (color online). Experimental setup.

puts, one at 532 nm to pump the parametric crystal, and the second at 1064 nm to generate the image that will be amplified and processed. In order to eliminate the technical excess noise, the 1064 nm beam is injected into a mode cleaning cavity. We have studied two different configurations: in the first one the nonlinear crystal is a type I $LiNbO_3$ crystal, inserted in a confocal cavity. In order to minimize the threshold of parametric oscillation, the cavity is doubly resonant on the pump mode and on the degenerate signal-idler mode. In the second configuration, shown in Fig. 1, the parametric crystal is a type II KTP crystal, and the cavity is triply resonant on the pump mode and on the signal and idler modes of the same frequencies but orthogonal polarizations. In order to make the tuning of the device to exact triple resonance easier, we have used a dual-cavity configuration [18,19] in which the pump field resonates in the cavity closed by the input mirror and the output face of the crystal, whereas the signal and idler modes resonate in another cavity, closed by the input face of the crystal and the output mirror, which can be independently tuned to resonance. Because the crystal has planar faces, these cavities cannot be confocal. We have therefore tuned them to the hemiconfocal configuration (in which the plane mirror is separated from the output curved mirror by a distance equal to a quarter of the radius of curvature of the mirror). In both configurations, the threshold for parametric oscillation using an optimally focused pump is about 30 mW. The waist of the pump cavity is then enlarged, so that the pump field can now amplify many transverse modes of the subharmonic cavity. In order to ensure the most stable possible operation of the system, the parametric crystal is temperature stabilized within a mK and all the different cavities are carefully stabilized using the Pound-Drever-Hall method.

An input image of desired shape is imaged on the input crystal face in an imaging transformation conserving both the amplitude and the phase of the image, and the relative phase between the pump and the input field is controlled by a mirror placed on a piezoelectric transducer. The properties of degenerate cavities in terms of transmission of images have been studied in [20]: a confocal cavity transmits either the odd or the even part of the input image, whereas a hemiconfocal cavity transmits only half of the even (or odd) transverse modes, and mixes the images with their spatial Fourier transform. The output infrared image is sent either to a CCD camera that records the image in the near or the far field, or to a detecting device measuring quantum fluctuations: in the type I configuration, it measures the fluctuations of the total intensity of the amplified image. In the type II configuration, a polarizing beam splitter separates the signal and idler polarizations' directions and allows us to measure independently the intensity fluctuations of the two polarization components of the amplified image. The photodetectors are InGaAs photodiodes with matched quantum efficiencies around 95%. These two detecting devices (CCD and photodetectors) allow for different characterization of the system: the CCD is here to control the imaging properties of the cavity, at low analysis frequency and in the classical regime. However, because of classical noise at these frequencies, the nonclassical character of these images is analyzed through high speed photodetectors at a few megahertz analysis frequency. These detectors do not resolve spatially the image but detect the entire incoming field, and thus both detecting schemes are necessary simultaneously.

Let us first briefly recall some properties of degenerate parametric amplification. In the type I configuration, the parametric amplifier is phase sensitive (PSA) and transforms an input coherent (or vacuum state) into a squeezed state. In the ideal lossless case, the signal-to-noise ratio is preserved in the amplification process. The noise factor F of the system, defined as the input signal-to-noise ratio divided by the output signal-to-noise ratio, is equal to 1, and the amplification is said to be "noiseless" [7]. Furthermore, if one takes into account the quantum efficiency of the detector this process can increase the overall signal-to-noise ratio [21]. In the type II configuration, the amplifier is a usual phase insensitive amplifier (PIA) if the input field is injected with the polarization of the signal or idler mode, and, as expected for a regular amplifier, the noise factor tends to 2 for high gains. The amplifier is phase sensitive and noiseless if the input field is injected with a polarization at 45° of the signal and idler mode polarizations. In the latter case, the system generates squeezed states in the output modes at 45° of the signal and idler polarizations, and also "quantum clones" [8], or EPR correlated beams on the signal and idler polarizations.

All these properties hold for single pass amplification and also for intracavity amplification with a single coupling mirror used both for input and output [22,23]. In the more practical scheme in which the input and output mirrors of the optical cavity are different, they are somehow modified because of the admixture of a new source of incoming vacuum fluctuations at the output mirror. In order to optimize the system for maximum squeezing and quantum correlations on the output beams, we have chosen the transmission of the input mirror to be very small compared to the transmission of the output mirror. This situation is not optimum for amplification as the input beam suffers significant insertion losses when it enters the cavity. The quantum character of the amplification process will then be assessed by comparing its experimental performances to a theoretical model taking into account such insertion losses. In this respect the most convenient parameter characteriz-

ing the amplifying device is its "on-off" noise factor F_{oo}, defined as the relative variation of the signal-to-noise ratio measured at the output when the amplifier pump field varies from its actual value (ampli "on") to zero (ampli "off"), which has been also measured in several other experiments [9,10]. Let us note that F_{oo} may be smaller than 1, meaning that the amplification process may improve a signal-to-noise ratio that has beforehand been degraded by the losses.

In the first configuration using a type I crystal, the input image was a strongly mismatched TEM_{00} mode, with a waist larger than the one of the eigenmode of the optical parametric amplifier (OPA) cavity. We observed gains in the PSA configuration of the order of 4. The signal to be amplified consists of a small modulation at 5 MHz of the total image intensity, and the noise is measured at the frequency of the modulation. It is then possible to determine the on-off noise factor F_{oo} defined above, and also to measure the "on-off gain" G_{oo} defined in the same way. One then gets experimental points of coordinates (G_{oo}, F_{oo}) which are plotted in Fig. 2. The same figure contains two theoretical curves: the upper one gives the variation of F_{oo} versus G_{oo} for a regular, phase insensitive, parametric amplifier, and the lower one gives F_{oo} for a phase sensitive, noiseless amplifier. Both curves have been calculated for the same experimental values of the input and output mirrors' transmission factors. One observes that the measured values of F_{oo} lie well below the PIA theoretical curve. This shows that the amplifier adds much less noise than a phase sensitive amplifier with the same losses, which is evidence that the device indeed operates in the quantum regime of noiseless amplification.

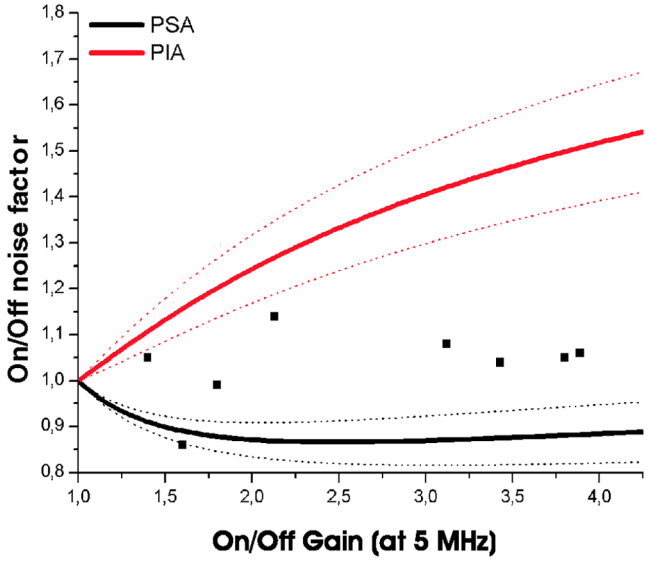

FIG. 2 (color online). Results in the confocal OPA. Dots: experimental values of on-off noise factor in function of the on-off gain. Full lines: theoretical values in the PIA and PSA cases. Dotted lines: uncertainty in the determination of the parameters used in the theory.

In the experiment with the type II crystal, we used different shapes of the input image: vertical slits or horizontal slits of different sizes as shown in Fig. 3, and unmatched TEM_{00} modes. The noise and the signal were measured on the sum of the high frequency channels of the signal and idler polarization photocurrents. The experimental results for the on-off noise factor are represented in Fig. 3. One observes again that the measured noise factors are very close to the PSA theoretical curve and well below the PIA theoretical curve: the system operates indeed in the regime of noiseless amplification.

In both experiments, one observes that the experimental values of F_{oo} (on which we did not make any postselection) vary significantly, and differ from the theory. This effect is not due to parameters we did not take into account in the theory, but to the varying quality of the locking, which is critical because of the strong thermal effects taking place inside the crystal. However, all our experimental data lie well inside the area corresponding to the quantum regime of image amplification. The type II experimental setup turned out to be less sensitive to temperature fluctuations than the type I experiment. This enabled us to study in more detail the quantum properties of the type II OPA. We measured the quantum fluctuations of the total intensity of the images at the output of the cavity, in either the amplification or the deamplification regime, with a digital acquisition system described in [24].

When the phase of the input image was stabilized on a value leading to image amplification (upper curve on Fig. 4), we observed that the noise on the difference between the total intensities of the signal and idler amplified images at a frequency of 5 MHz was well below the shot noise level, showing that the system generated quantum correlated "twin images." The observed reduction factor was 30% with respect to the shot noise level, roughly

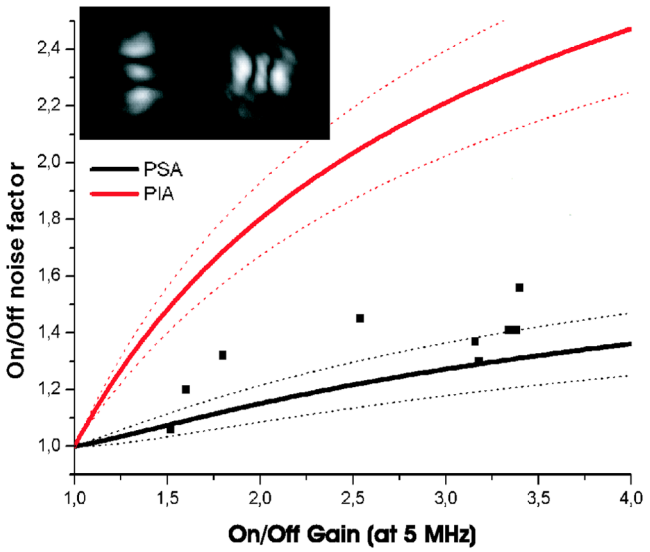

FIG. 3 (color online). Results in the hemiconfocal OPA. Same curves as Fig. 2. The images above are typical images used in our amplification experiments.

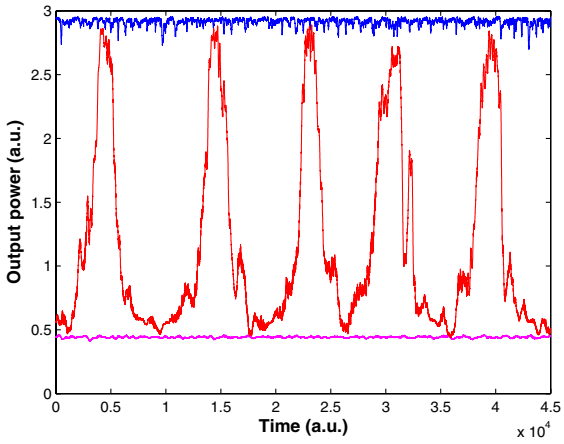

FIG. 4 (color online). Temporal variations of the output signal power of the optical parametric oscillator in three regimes: when the relative phase between the signal and the pump is scanned, and locked in the amplification or deamplification regime. When locked our amplifier was stable during a few minutes.

independent of the shape of the input images, and in fair agreement with theory (predicting a quantum noise reduction of 45%). Our setup thus operates as a "quantum cloning amplifier" of images [25], an extension of the "quantum cloning amplifier" of simple TEM_{00} beams demonstrated in [8].

When the phase of the input image was stabilized on a value leading to image deamplification (lower curve on Fig. 4), we observed that the noise on the sum of the total intensities of the signal and idler deamplified images was also well below the shot noise level, showing that the system generated in this case an intensity-squeezed image on the polarization at 45 from the signal and idler polarizations. Again, the observed reduction factor was 30% below shot noise. To the best of our knowledge, this is the first experimental evidence of generation of a nonclassical image of complex shape. This shows that we are able to tailor the total quantum fluctuations of a light beam of any shape resonating in the cavity, a feature that can be very useful in multipixel processing [3].

In conclusion, we have experimentally demonstrated in this Letter significant quantum effects in cw amplification of images of different shapes, namely, the generation of quantum intensity correlated images, or of amplitude squeezed images. Our image amplifier, though affected by strong insertion losses, was shown to operate in the noiseless regime. If one actually wants to use such a noiseless device in practical applications, it is, however, necessary to modify the setup, optimized for squeezing and not for noiseless amplification. This can be achieved in principle by using an impedance matched cavity for which there is no reflected beam at the input mirror of the cavity. Calculations show that in our present experimental configuration, an OPA with a ratio between the input coupler transmission and output coupler transmission of $1/4$ would be effectively noiseless for gains comprised between 4 and 10, with cavity thresholds comparable to our setup and with negligible reflected power from the cavity.

We have also shown that it is possible to modify the quantum fluctuations of images of various shapes with the same experimental setup, so that it is in principle possible to quickly switch from one squeezed image to another. This is what is needed, for example, in the optical readout of optical memories below the standard quantum limit [5]. The present setups, however, based on hemiconfocal or confocal cavities, are so far not able to process nonclassical images of any shape. We are presently developing a setup using a self-imaging cavity [26] that will not be hampered by this restriction. This new device will also enable us to investigate "local" quantum effects, which have been predicted for measurements performed not on the total intensity but on the different pixels of a CCD camera recording the image [27,28].

[1] J. Preskill, J. Mod. Opt. **47**, 127 (2000).
[2] *Quantum Imaging*, edited by M. Kolobov (Springer-Verlag, Berlin, 2006); A. Gatti, E. Brambilla, and L. Lugiato, Prog. Opt. (to be published); (to be published).
[3] N. Treps *et al.*, Phys. Rev. A **71**, 013820 (2005).
[4] N. Treps *et al.*, Science **301**, 940 (2003).
[5] V. Delaubert *et al.*, Phys. Rev. A **73**, 013820 (2006).
[6] M. T. L. Hsu *et al.*, IEEE J. Quantum Electron. **42**, 1001 (2006).
[7] C. M. Caves, Phys. Rev. D **26**, 1817 (1982).
[8] J. A. Levenson *et al.*, Phys. Rev. Lett. **70**, 267 (1993).
[9] S. K. Choi, M. Vasilyev, and P. Kumar, Phys. Rev. Lett. **83**, 1938 (1999).
[10] A. Mosset, F. Devaux, and E. Lantz, Phys. Rev. Lett. **94**, 223603 (2005).
[11] C. F. McCormick, V. Boyer, E. Arimondo, and P. D. Lett, Opt. Lett. 32, 178 (2007).
[12] V. Josse *et al.*, Phys. Rev. Lett. **96**, 163602 (2006).
[13] L. A. Wu, H. J. Kimble, J. Hall, and H. Wu, Phys. Rev. Lett. **57**, 2520 (1986).
[14] K. Schneider *et al.*, Opt. Lett. **21**, 1396 (1996).
[15] J. Laurat *et al.*, Phys. Rev. A **70**, 042315 (2004).
[16] Z. Y. Ou, S. F. Pereira, and H. J. Kimble, Phys. Rev. Lett. **70**, 3239 (1993).
[17] Very recently squeezed TEM_{01} and TEM_{02} Hermite-Gauss modes have been generated: M. Lassen *et al.*, J. Eur. Opt. Soc. **1**, 06003 (2006).
[18] S. Gigan *et al.*, J. Mod. Opt. **53**, 809 (2006).
[19] B. Scherrer *et al.*, J. Opt. Soc. Am. B **17**, 1716 (2000).
[20] S. Gigan *et al.*, Phys. Rev. A **72**, 023804 (2005).
[21] K. Bencheikh *et al.*, Appl. Phys. Lett. **66**, 399 (1995).
[22] M. Kolobov and L. Lugiato, Phys. Rev. A **52**, 4930 (1995).
[23] S. Mancini, A. Gatti, and L. A. Lugiato, Eur. Phys. J. D **12**, 499 (2000).
[24] M. Martinelli *et al.*, Phys. Rev. A **67**, 023808 (2003).
[25] P. Navez, E. Brambilla, A. Gatti, and L. A. Lugiato, Phys. Rev. A **65**, 013813 (2001).
[26] J. A. Arnaud, Appl. Opt. **8**, 189 (1969).
[27] L. Lopez *et al.*, Phys. Rev. A **67**, 023808 (2005).
[28] A. Gatti *et al.*, Eur. Phys. J. D **30**, 123 (2004).